

Kinetic Modeling of Polymerization of Butadiene Using Cobalt-Based Ziegler–Natta Catalyst

SINGGIH NITIRAHARDJO,¹ SUNGGYU LEE,^{*1} and JOSEPH W. MILLER, JR.²

¹Department of Chemical Engineering, The University of Akron, Akron, Ohio 44325, and ²Chemical Research & Development, The Goodyear Tire & Rubber Company, Akron, Ohio 44306

SYNOPSIS

The reaction mechanism and subsequent kinetics for polymerization of butadiene using cobalt-based Ziegler–Natta catalysts have been investigated by many researchers. Kinetic models developed from these investigations can be used to predict the monomer conversion quite accurately; however, it is difficult to develop models that accurately predict the molecular weight as a function of time or conversion. In this paper, an attempt is made to model the reaction mechanism for the polymerization of butadiene using the cobalt octoate/diethyl aluminum chloride/water catalyst system with data taken from the literature. A dual active site mechanism is proposed and incorporated in a kinetic model. In this case, all reaction steps except the formation of byproducts step have two rate constants. The simulation results predict the molecular weight as a function of conversion and time better than results from previously published models.

INTRODUCTION

A good deal of interesting work has been done on the polymerization of butadiene initiated by Ziegler–Natta catalysts. Many researchers have tried to obtain a better understanding of the structure and the polymerization mechanism. Having better knowledge of the polymerization mechanism is a very important step in the development of effective design and control systems for polymerization reactors. However, the knowledge of the catalyst structure and polymerization mechanism of Ziegler–Natta catalysts is still very limited because of the complexity of the catalyst system.

Many investigators have tried to develop mathematical models, but most of them have found limited applicability because their range of investigation is limited to relatively low conversion and molecular weights. Accordingly, it is aimed, in this study, to develop models of greater practicality. The developed models will describe the conversion versus time and molecular weights versus conversion for poly-

merization of butadiene by cobalt-based Ziegler–Natta catalysts. The experimental data are obtained from Honig's work¹ and the values of kinetic constants are obtained from Honig et al.²

MECHANISM OF POLYMERIZATION

Many investigators have developed various mathematical models for cobalt-based Ziegler–Natta polymerization of butadiene. A summary of those papers is shown in Table I. Most of those models were based on curve fitting techniques and modeling of molecular weights was omitted in most instances.

A substantial improvement in kinetic analysis and modeling was published by Honig et al.² based on the experimental work of Honig.^{1,6} Honig rigorously studied the catalyst system, cobalt octoate/diethyl aluminum chloride (DEAC)/water. The kinetic model, summarized in Table II, predicts conversion versus time quite well, but their predictions for molecular weight, especially the weight average molecular weight, is grossly underestimated at higher conversion or at longer time. Their mathematical model and simulation have been reproduced and the simulation results for molecular weights

* To whom correspondence should be addressed.

Table I Published Rate Equations in the Polymerization of Butadiene Using Cobalt-Based Ziegler–Natta Catalysts

Catalyst System	Rate Equation	Ref.
$\text{CoCl}_2 \cdot 4\text{C}_5\text{H}_5\text{N}/\text{Et}_2\text{AlCl}/\text{H}_2\text{O}$	$\ln \frac{[\text{M}]_0}{[\text{M}]} = \frac{k_p k_c [\text{Co}]_i}{k_c - k_t} \left\{ \frac{1}{k_t} [1 - \exp(-k_t t)] - \frac{1}{k_c} [1 - \exp(-k_c t)] \right\}$	Hsu ³
$\text{Co}(\text{acac})_3/(i\text{-Bu})_3\text{Al}/\text{H}_2\text{O}$	$\ln \frac{[\text{M}]_0}{[\text{M}]} = \frac{k_p [\text{C}^*]}{k_c [\text{C}^*]_0} \ln(1 + k_c [\text{C}^*]_0 t)$	Yang ⁴
$\text{Co}(\text{acac})_3/\text{Et}_2\text{AlCl}/\text{H}_2\text{O}$	$\ln \frac{[\text{M}]_0}{[\text{M}]} = k_p \quad (T < 25^\circ\text{C})$ $= \frac{k_p}{k_t} \ln(1 + k_t [\text{C}^*]_0 t) \quad (T > 25^\circ\text{C})$	Honig ²
$\text{CoF}_2/\text{Et}_3\text{Al}_2\text{Cl}_3$	$R_p = k[\text{Co}][\text{M}]^2$	Honig ²
$\text{CoCl}_2 \cdot 4\text{Py}/\text{Et}_2\text{AlCl}/\text{H}_2\text{O}$	$\ln \frac{[\text{M}]_i}{[\text{M}]} = \frac{k_p [\text{Co}^*]_i}{k_{tc}([\text{Co}^*]_i)} \ln(1 + k_{tc}[\text{Co}^*]_i t)$	Ho ⁵

versus time can be seen in Figure 1. The rate constants that are used for this model are the same as the values in Honig's paper. These values are shown in a later section.

Since their mathematical model is not adequate especially in predicting the molecular weights, a better model is required. A possible improvement in modeling is incorporating two active sites. Some investigators have tried to model the two active site scheme; however, their models have been either for different catalyst systems or only for low conversion. Two papers published by Lee and Hsu^{7,8} are examples, in which they tried to model the polymerization of butadiene in toluene using nickel(II) stearate–diethyl aluminum chloride catalyst. Another example is a paper by Medvedev et al.⁹ for a system of $\text{CoCl}_2 \cdot (\text{C}_5\text{H}_5\text{N}) - \text{AlR}_2\text{Cl} - \text{H}_2\text{O}$ catalyst.

Recently, Roffel¹⁰ also proposed a double site model for Cobalt based Ziegler–Natta catalyst. In his derivation, he developed a dynamic polymerization model. However, a detailed comparison between his simulation results and experimental results for molecular weights versus time or versus conversion was not shown.

This paper also uses a two active site model which is an extension of Honig's single active site model and is also different from Roffel's model. The difference from Honig's model is that instead of using a single active site, a two active site mechanism system is used. The differences between this model and Roffel's model are the use of active site termination by chain transfer to promoter (water) and the concept of chain transfer to butene-1 and regeneration of active sites.

Table II The Reaction Scheme for Single Active Site Reaction from Honig² a

Reaction Step	Reaction	Rate Constant
Initiation (formation of active site)	$\text{Co} + \text{Al} + \text{H}_2\text{O} \rightarrow \text{C}^*$	k_i
Initiation	$\text{C}^* + \text{M} \rightarrow \text{C}^*\text{P}_1$	k_p
Formation of byproducts	$\text{Co} + \text{Al} + \text{H}_2\text{O} \rightarrow \text{E}_b$	k_a
Propagation	$\text{C}^*\text{P}_r + \text{M} \rightarrow \text{C}^*\text{P}_{r+1}$	k_p
Transfer to monomer	$\text{C}^*\text{P}_r + \text{M} \rightarrow \text{C}^*\text{P}_1 + \text{Q}_r$	k_c
Transfer to 1-butene	$\text{C}^*\text{P}_r + \text{B} \rightarrow \text{C}^*\text{B} + \text{Q}_r$	k_b
Regeneration of active sites	$\text{C}^*\text{B} + \text{M} \rightarrow \text{C}^*\text{P}_1 + \text{B}$	k_z
Catalyst deactivation	$\text{C}^*\text{P}_r \rightarrow \text{Q}_r + \text{C}$	k_t

^a Co = cobalt octoate, Al = diethylaluminum chloride; C* = active catalyst site, E_b = catalyst byproduct, M = butadiene monomer, C*P₁ = growing chain of unit length, C*P_r = growing chain of length r, C*B = short-lived 1-butene/catalyst complex, Q_r = dead polymer chain of length r, B = 1-butene, and C = deactivated catalyst site.

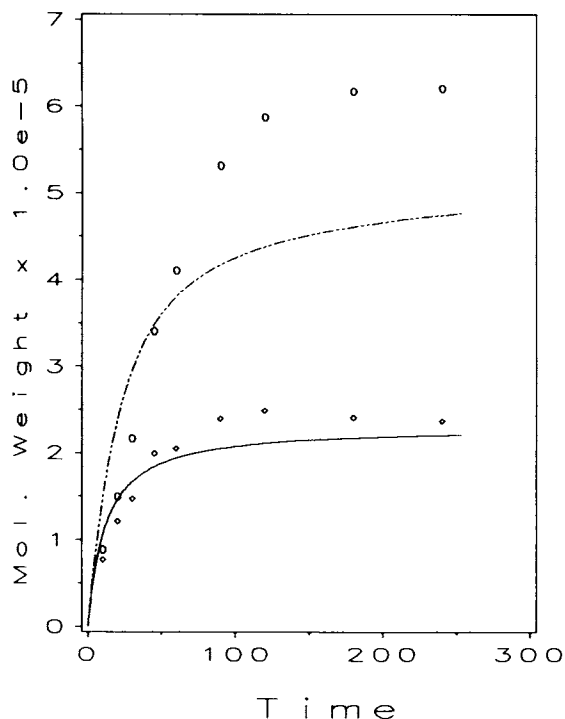


Figure 1 Molecular weights versus time for single active site model for $[Co] = 0.000125M$, $[M]_0 = 1.43M$, $T = 15^\circ C$ and $FE = 0.25$: (O) M_w from experimental data (1); (\diamond) M_n from experimental data (1); (- · - ·) M_w from simulation results; (—) M_n from simulation results.

In the case of dual active sites that will be discussed in this paper, the reactivity of each active site is different. Therefore, except for the formation of byproducts step, there will be two rate constants for each reaction step. The proposed mechanism scheme for cobalt octoate/diethyl aluminum chloride/water catalyst system is shown in Table III.

DEVELOPMENT OF KINETIC MODEL

In order to obtain expressions for conversion and molecular weights based on the proposed mechanism (two active sites), some kinetic expressions have to be derived. All the assumptions that will be used in these derivations are as follows:

- monomer consumption other than propagation is negligible;
- concentration of Al-alkyl and water does not affect molecular weights^{2,6};
- quasi-steady-state assumption (QSSA) for both active catalyst species and the 1-butene/catalyst complex.

The rate expression for cobalt octoate catalyst is

$$\frac{d[Co]}{dt} = -(k_{i1} + k_{i2})[Co]^m[Al]^n[H_2O]^p - k_s[Co]^r[Al]^s[H_2O]^t \quad (1)$$

Table III The Reaction Mechanism for Dual Active Sites

Reaction Step	Reaction	Rate Const
Initiation (formation of active site)	$Co + Al + H_2O \rightarrow C_1^*$	k_{i1}
	$Co + Al + H_2O \rightarrow C_2^*$	k_{i2}
Initiation	$C_1^* + M \rightarrow C_1^*P_1$	k_{p1}
	$C_2^* + M \rightarrow C_2^*P_1$	k_{p2}
Formation of byproducts	$Co + Al + H_2O \rightarrow E_b$	k_s
Propagation	$C_1^*P_r + M \rightarrow C_1^*P_{r+1}$	k_{p1}
	$C_2^*P_r + M \rightarrow C_2^*P_{r+1}$	k_{p2}
Transfer to monomer	$C_1^*P_r + M \rightarrow C_1^*P_1 + Q_r$	k_{c1}
	$C_2^*P_r + M \rightarrow C_2^*P_1 + Q_r$	k_{c2}
Transfer to 1-butene	$C_1^*P_r + B \rightarrow C_1^*B + Q_r$	k_{b1}
	$C_2^*P_r + B \rightarrow C_2^*B + Q_r$	k_{b2}
Regeneration of active sites	$C_1^*B + M \rightarrow C_1^*P_1 + B$	k_{z1}
	$C_2^*B + M \rightarrow C_2^*P_1 + B$	k_{z2}
Catalyst deactivation	$C_1^*P_r \rightarrow Q_r + C_1$	k_{d1}
	$C_2^*P_r \rightarrow Q_r + C_2$	k_{d2}

* C_1^* = active catalyst site 1, C_2^* = active catalyst site 2, $C_1^*P_1$ = growing chain of unit length with active site #1, $C_2^*P_1$ = growing chain of unit length with active site #2, $C_1^*P_r$ = growing chain of length r with active site #1, $C_2^*P_r$ = growing chain of length r with active site #2, C_1^*B = short-lived 1-butene/catalyst complex with active site #1, C_2^*B = short-lived 1-butene/catalyst complex with active site #2, C_1 = deactivated catalyst site with active site #1, and C_2 = deactivated catalyst site with active site #2.

Applying assumption (b), eq. (1) can be simplified to

$$\frac{d[\text{Co}]}{dt} = -\{k_{i1} + k_{i2}\}[\text{Co}]^m - k_s[\text{Co}]^r \quad (2)$$

The two active sites initially formed are described by the following rate expressions:

$$\frac{d[\text{C}_1^*]}{dt} = k_{i1}[\text{Co}]^m[\text{Al}]^n[\text{H}_2\text{O}]^p - k_{p1}[\text{C}_1^*][\text{M}] \quad (3)$$

$$\frac{d[\text{C}_2^*]}{dt} = k_{i2}[\text{Co}]^m[\text{Al}]^n[\text{H}_2\text{O}]^p - k_{p2}[\text{C}_2^*][\text{M}] \quad (4)$$

Using the same assumption (concentration of aluminum alkyl and water does not affect the molecular weights), eqs. (3) and (4) become

$$\frac{d[\text{C}_1^*]}{dt} = k_{i1}[\text{Co}]^m - k_{p1}[\text{C}_1^*][\text{M}] \quad (5)$$

$$\frac{d[\text{C}_2^*]}{dt} = k_{i2}[\text{Co}]^m - k_{p2}[\text{C}_2^*][\text{M}] \quad (6)$$

Applying the quasi-steady-state assumption (QSSA), eq. (5) becomes

$$[\text{C}_1^*] = \frac{k_{i1}[\text{Co}]^m}{k_{p1}[\text{M}]} \quad (7)$$

and eq. (6) becomes

$$[\text{C}_2^*] = \frac{k_{i2}[\text{Co}]^m}{k_{p2}[\text{M}]} \quad (8)$$

The rate expressions for short-lived 1-butene/catalyst complex are

$$\frac{d[\text{C}_1^*\text{B}]}{dt} = k_{b1}[\text{C}_1^*\text{P}][\text{B}] - k_{z1}[\text{C}_1^*\text{B}][\text{M}] \quad (9)$$

$$\frac{d[\text{C}_2^*\text{B}]}{dt} = k_{b2}[\text{C}_2^*\text{P}][\text{B}] - k_{z2}[\text{C}_2^*\text{B}][\text{M}] \quad (10)$$

After applying the QSSA, these equations become

$$[\text{C}_1^*\text{B}] = \frac{k_{b1}[\text{B}][\text{C}_1^*\text{P}]}{k_{z1}[\text{M}]} \quad (11)$$

$$[\text{C}_2^*\text{B}] = \frac{k_{b2}[\text{B}][\text{C}_2^*\text{P}]}{k_{z2}[\text{M}]} \quad (12)$$

The monomer consumption is described by the following kinetic expression:

$$\begin{aligned} \frac{d[\text{M}]}{dt} = & -k_{p1}[\text{M}]\{[\text{C}_1^*] + [\text{C}_1^*\text{P}]\} \\ & - k_{p2}[\text{M}]\{[\text{C}_2^*] + [\text{C}_2^*\text{P}]\} \\ & - [\text{M}]\{k_{z1}[\text{C}_1^*\text{B}] + k_{z2}[\text{C}_2^*\text{B}]\} \\ & - k_{c1}[\text{M}][\text{C}_1^*\text{P}] - k_{c2}[\text{M}][\text{C}_2^*\text{P}] \quad (13) \end{aligned}$$

Applying assumption (a), eq. (13) can be written as

$$\frac{d[\text{M}]}{dt} = -\{k_{p1}[\text{C}_1^*\text{P}] + k_{p2}[\text{C}_2^*\text{P}]\}[\text{M}] \quad (14)$$

The rate expressions for $[\text{C}_1^*\text{P}_1]$ and $[\text{C}_2^*\text{P}_1]$ are given by

$$\begin{aligned} \frac{d[\text{C}_1^*\text{P}_1]}{dt} = & k_{p1}[\text{M}][\text{C}_1^*] - k_{p1}[\text{M}][\text{C}_1^*\text{P}_1] \\ & + k_{c1}[\text{M}][\text{C}_1^*\text{P}] + k_{z1}[\text{M}][\text{C}_1^*\text{B}] \\ & - k_{c1}[\text{M}][\text{C}_1^*\text{P}_1] - k_{b1}[\text{C}_1^*\text{P}_1][\text{B}] \\ & - k_{t1}[\text{C}_1^*\text{P}_1] \quad (15) \end{aligned}$$

$$\begin{aligned} \frac{d[\text{C}_2^*\text{P}_1]}{dt} = & k_{p2}[\text{M}][\text{C}_2^*] - k_{p2}[\text{M}][\text{C}_2^*\text{P}_1] \\ & + k_{c2}[\text{M}][\text{C}_2^*\text{P}] + k_{z2}[\text{M}][\text{C}_2^*\text{B}] \\ & - k_{c2}[\text{M}][\text{C}_2^*\text{P}_1] - k_{b2}[\text{C}_2^*\text{P}_1][\text{B}] \\ & - k_{t2}[\text{C}_2^*\text{P}_1] \quad (16) \end{aligned}$$

Applying the assumptions, eqs. (15) and (16) become

$$\begin{aligned} \frac{d[\text{C}_1^*\text{P}_1]}{dt} = & k_{i1}[\text{Co}]^m - k_{p1}[\text{M}][\text{C}_1^*\text{P}_1] \\ & + k_{c1}[\text{M}][\text{C}_1^*\text{P}] + k_{b1}[\text{B}][\text{C}_1^*\text{P}] \\ & - k_{c1}[\text{M}][\text{C}_1^*\text{P}_1] - k_{b1}[\text{C}_1^*\text{P}_1][\text{B}] \\ & - k_{t1}[\text{C}_1^*\text{P}_1] \quad (17) \end{aligned}$$

$$\begin{aligned} \frac{d[\text{C}_2^*\text{P}_1]}{dt} = & k_{i2}[\text{Co}]^m - k_{p2}[\text{M}][\text{C}_2^*\text{P}_1] \\ & + k_{c2}[\text{M}][\text{C}_2^*\text{P}] + k_{b2}[\text{B}][\text{C}_2^*\text{P}] \\ & - k_{c2}[\text{M}][\text{C}_2^*\text{P}_1] - k_{b2}[\text{C}_2^*\text{P}_1][\text{B}] \\ & - k_{t2}[\text{C}_2^*\text{P}_1] \quad (18) \end{aligned}$$

The sum of eqs. (15) and (16) gives the expression for total living polymer having chain length of 1:

$$\begin{aligned} \frac{d[C_1^*P_1]}{dt} = & k_{p1}[M][C_1^*] - k_{p1}[M][C_1^*P_1] \\ & + k_{c1}[M][C_1^*P] + k_{z1}[M][C_1^*B] \\ & - k_{c1}[M][C_1^*P_1] - k_{b1}[C_1^*P_1][B] \\ & - k_{t1}[C_1^*P_1] + k_{p2}[M][C_2^*] \\ & - k_{p2}[M][C_2^*P_1] + k_{c2}[M][C_2^*P] \\ & + k_{z2}[M][C_2^*B] - k_{c2}[M][C_2^*P_1] \\ & - k_{b2}[C_2^*P_1][B] - k_{t2}[C_2^*P_1] \quad (19) \end{aligned}$$

The rate expressions for $[C_1^*P_r]$ and $[C_2^*P_r]$ are given by

$$\begin{aligned} \frac{d[C_1^*P_r]}{dt} = & k_{p1}[M][C_1^*P_{r-1}] \\ & - k_{p1}[M][C_1^*P_r] - k_{c1}[M][C_1^*P_r] \\ & - k_{b1}[C_1^*P_r][B] - k_{t1}[C_1^*P_r] \quad (20) \end{aligned}$$

$$\begin{aligned} \frac{d[C_2^*P_r]}{dt} = & k_{p2}[M][C_2^*P_{r-1}] \\ & - k_{p2}[M][C_2^*P_r] - k_{c2}[M][C_2^*P_r] \\ & - k_{b2}[C_2^*P_r][B] - k_{t2}[C_2^*P_r] \quad (21) \end{aligned}$$

Adding eq. (15) to the sum of eq. (20) over $r = 2$ to infinity gives the following expression for the zeroth moment for site 1:

$$\begin{aligned} \frac{dY_{01}}{dt} = & k_{p1}[M][C_1^*] + k_{z1}[M][C_1^*B] \\ & - k_{b1}[C_1^*P][B] - k_{t1}[C_1^*P] \quad (22) \end{aligned}$$

Applying the assumptions, eq. (22) becomes

$$\frac{dY_{01}}{dt} = k_{i1}[Co]^m - k_{t1}Y_{01} \quad (23)$$

Similarly, by adding eq. (16) to the sum of eq. (21) over $r = 2$ to infinity and then applying the assumptions gives

$$\begin{aligned} \frac{dY_{02}}{dt} = & k_{p2}[M][C_2^*] + k_{z2}[M][C_2^*B] \\ & - k_{b2}[C_2^*P][B] - k_{t2}[C_2^*P] \quad (24) \end{aligned}$$

$$\frac{dY_{02}}{dt} = k_{i2}[Co]^m - k_{t2}Y_{02} \quad (25)$$

The first moment for each active site can also be obtained by adding the $[C_i^*P_1]$ to the sum of $r[C_i^*P_r]$ over $r = 2$ to infinity. Performing this and applying assumptions yield

$$\begin{aligned} \frac{dY_{11}}{dt} = & k_{p1}[M][C_1^*] + k_{p1}[M]Y_{01} \\ & + k_{c1}[M]\{Y_{01} - Y_{11}\} - k_{b1}[B]Y_{11} \\ & + k_{z1}[M][C_1^*B] - k_{t1}Y_{11} \quad (26) \end{aligned}$$

$$\begin{aligned} = & k_{i1}[Co]^m + k_{p1}[M]Y_{01} \\ & + k_{c1}[M]\{Y_{01} - Y_{11}\} \\ & + k_{b1}[B]\{Y_{01} - Y_{11}\} - k_{t1}Y_{11} \quad (27) \end{aligned}$$

$$\begin{aligned} \frac{dY_{12}}{dt} = & k_{p2}[M][C_2^*] + k_{p2}[M]Y_{02} \\ & + k_{c2}[M]\{Y_{02} - Y_{12}\} - k_{b2}[B]Y_{12} \\ & + k_{z2}[M][C_2^*B] - k_{t2}Y_{12} \quad (28) \end{aligned}$$

$$\begin{aligned} = & k_{i2}[Co]^m + k_{p2}[M]Y_{02} \\ & + k_{c2}[M]\{Y_{02} - Y_{12}\} \\ & + k_{b2}[B]\{Y_{02} - Y_{12}\} - k_{t2}Y_{12} \quad (29) \end{aligned}$$

The rate expression for dead polymer having chain length of r is given by

$$\begin{aligned} \frac{d[Q_r]}{dt} = & k_{c1}[M][C_1^*P_r] + k_{c2}[M][C_2^*P_r] \\ & + k_{b1}[C_1^*P_r][B] + k_{b2}[C_2^*P_r][B] \\ & + k_{t1}[C_1^*P_r] + k_{t2}[C_2^*P_r] \quad (30) \end{aligned}$$

The rate expression for total (live + dead) polymer having length of r is given by

$$[P_r] = [C_1^*P_r] + [C_2^*P_r] + [Q_r] \rightarrow \begin{array}{l} \text{total (live + dead)} \\ \text{polymer having} \\ \text{length of } r \end{array}$$

$$\begin{aligned} \frac{d[P_r]}{dt} = & k_{p1}[M][C_1^*P_{r-1}] - k_{p1}[M][C_1^*P_r] \\ & + k_{p2}[M][C_2^*P_{r-1}] - k_{p2}[M][C_2^*P_r] \quad (31) \end{aligned}$$

Now, the moments for total polymer (live + dead) can be obtained.

0th moment: Adding eq. (19) to the sum of $[P_r]$ over $r = 2$ to infinity and then applying the assumptions gives

Table IV Differential Equations and Initial Condition for Dual Active Sites Model

<i>i</i>	Y_i	Diff. Equation No.	Initial Condition
1	M	14	$[M]_0 - FE [Co]'$
2	$C_1^*P_1$	17	$FE F1 [Co]'$
3	$C_2^*P_1$	18	$FE (1 - F1) [Co]'$
4	Y_{01}	23	$FE F1 [Co]'$
5	Y_{02}	25	$FE (1 - F1) [Co]'$
6	Y_{11}	27	$FE F1 [Co]'$
7	Y_{12}	29	$FE (1 - F1) [Co]'$
8	X_0	33	$FE [Co]'$
9	X_1	35	$FE [Co]'$
10	X_2	37	$FE [Co]'$

* $[Co]'$ is the initial (total) concentration of Co. The initial condition is based on the assumption that the initiation steps are instantaneous. Hence, all Co is reacted to form $C_1^*P_1$, $C_2^*P_1$, or byproduct at $t = 0$. $\rightarrow [Co] = 0$ in the differential equations. FE is a fraction of all Co that forms active centers. F1 is a fraction of active centers that are first type active center.

$$\begin{aligned} \frac{dX_0}{dt} &= k_{p1}[M][C_1^*] + k_{c1}[M]Y_{01} \\ &+ k_{z1}[M][C_1^*B] - k_{c1}[M][C_1^*P_1] \\ &- k_{b1}[B][C_1^*P_1] - k_{t1}[C_1^*P_1] \\ &+ k_{p2}[M][C_2^*] + k_{c2}[M]Y_{02} \\ &+ k_{z2}[M][C_2^*B] - k_{c2}[M][C_2^*P_1] \\ &- k_{b2}[B][C_2^*P_1] - k_{t2}[C_2^*P_1] \quad (32) \end{aligned}$$

$$\begin{aligned} &= k_{i1}[Co]^m + k_{c1}[M]Y_{01} + k_{b1}[B]Y_{01} \\ &- k_{c1}[M][C_1^*P_1] - k_{b1}[B][C_1^*P_1] \\ &- k_{t1}[C_1^*P_1] + k_{i2}[Co]^m + k_{c2}[M]Y_{02} \\ &+ k_{b2}[B]Y_{02} - k_{c2}[M][C_2^*P_1] \\ &- k_{b2}[B][C_2^*P_1] - k_{t2}[C_2^*P_1] \quad (33) \end{aligned}$$

1st moment: Adding eq. (19) to the sum of $r[P_r]$ over $r = 2$ to infinity gives

$$\begin{aligned} \frac{dX_1}{dt} &= k_{p1}[M][C_1^*] + k_{c1}[M]Y_{01} \\ &+ k_{z1}[M][C_1^*B] - k_{c1}[M][C_1^*P_1] \\ &- k_{b1}[B][C_1^*P_1] - k_{t1}[C_1^*P_1] \\ &+ k_{p1}[M]Y_{01} + k_{p2}[M][C_2^*] \\ &+ k_{c2}[M]Y_{02} + k_{z2}[M][C_2^*B] \end{aligned}$$

$$\begin{aligned} &- k_{c2}[M][C_2^*P_1] - k_{b2}[B][C_2^*P_1] \\ &- k_{t2}[C_2^*P_1] + k_{p2}[M]Y_{02} \quad (34) \end{aligned}$$

$$= \frac{dX_0}{dt} + k_{p1}[M]Y_{01} + k_{p2}[M]Y_{02} \quad (35)$$

2nd moment: Adding eq. (19) and the sum of $r^2[P_r]$ over $r = 2$ to infinity gives

$$\begin{aligned} \frac{dX_2}{dt} &= k_{p1}[M][C_1^*] + k_{c1}[M]Y_{01} \\ &+ k_{z1}[M][C_1^*B] - k_{c1}[M][C_1^*P_1] \\ &- k_{b1}[B][C_1^*P_1] - k_{t1}[C_1^*P_1] \\ &+ k_{p1}[M]\{Y_{01} + 2Y_{11}\} + k_{p2}[M][C_2^*] \\ &+ k_{c2}[M]Y_{02} + k_{z2}[M][C_2^*B] \\ &- k_{c2}[M][C_2^*P_1] - k_{b2}[B][C_2^*P_1] \\ &- k_{t2}[C_2^*P_1] + k_{p2}[M]\{Y_{02} + 2Y_{12}\} \quad (36) \end{aligned}$$

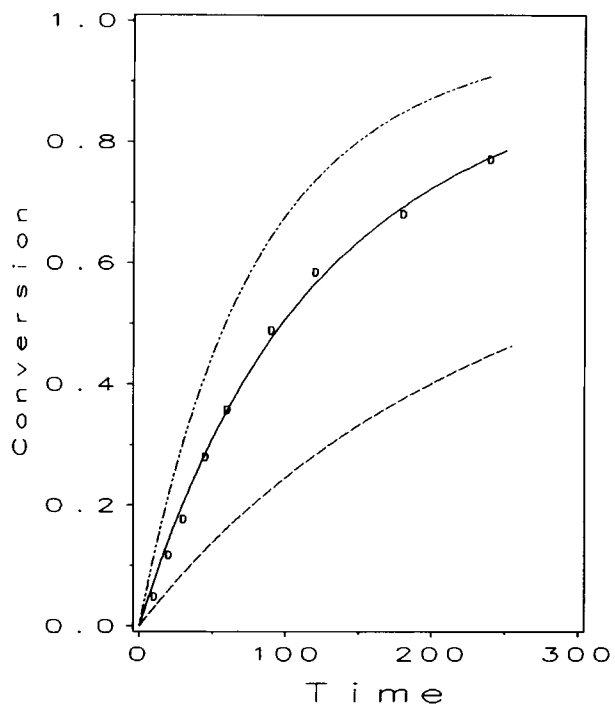


Figure 2 Conversion versus time for two active sites model for different values of FE. All other parameters are kept constant at $[Co] = 0.000125M$, $[M]_0 = 1.43M$, $T = 15^\circ C$, $F1 = 0.15$, $FF1 = 2.25$, and $FFT = 1.0$: (D) conv. from experimental data (1); (---) conv. from simulation results for $FE = 0.10$; (—) conv. from simulation results for $FE = 0.25$; (- · - ·) conv. from simulation results for $FE = 0.40$.

$$= \frac{dX_0}{dt} + k_{p1}[M]\{Y_{01} + 2Y_{11}\} + k_{p2}[M]\{Y_{02} + 2Y_{12}\} \quad (37)$$

Finally, the number and weight-average molecular weights can be calculated by using the following equations:

$$M_n = M_m \frac{X_1}{X_0} \quad (38)$$

$$M_w = M_m \frac{X_2}{X_1} \quad (39)$$

where M_N = number-average molecular weight, M_w = weight-average molecular weight, and M_m = monomer molecular weight.

NUMERICAL METHOD AND THE SYSTEM OF DIFFERENTIAL EQUATIONS

A semi-implicit third-order Runge-Kutta algorithm by Michelsen¹¹ is used to solve the system of differ-

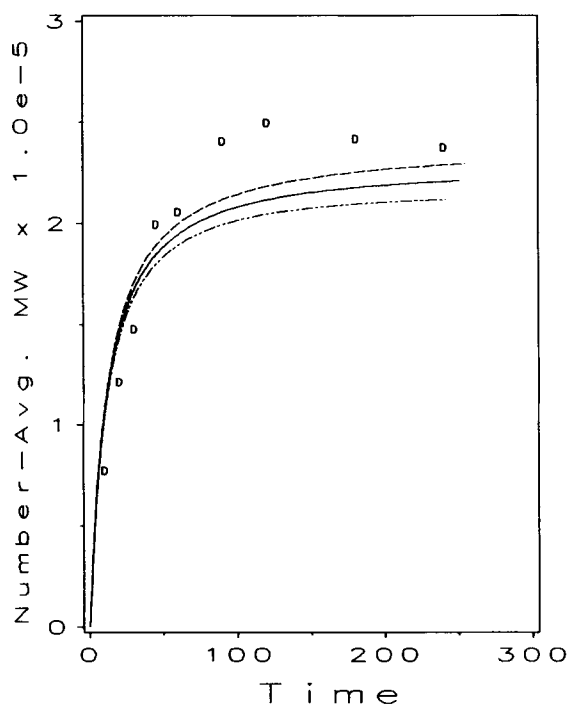


Figure 3 Number-averaged molecular weight versus time for two active sites model for different values of FE. All other parameters are kept constant at $[Co] = 0.000125M$, $[M]_0 = 1.43M$, $T = 15^\circ C$, $F1 = 0.15$, $FFI = 2.25$, and $FFT = 1.0$: (D) M_n from experimental data (1); (---) M_n from simulation results for FE = 0.10; (—) M_n from simulation results for FE = 0.25; (- · - ·) M_n from simulation results for FE = 0.40.

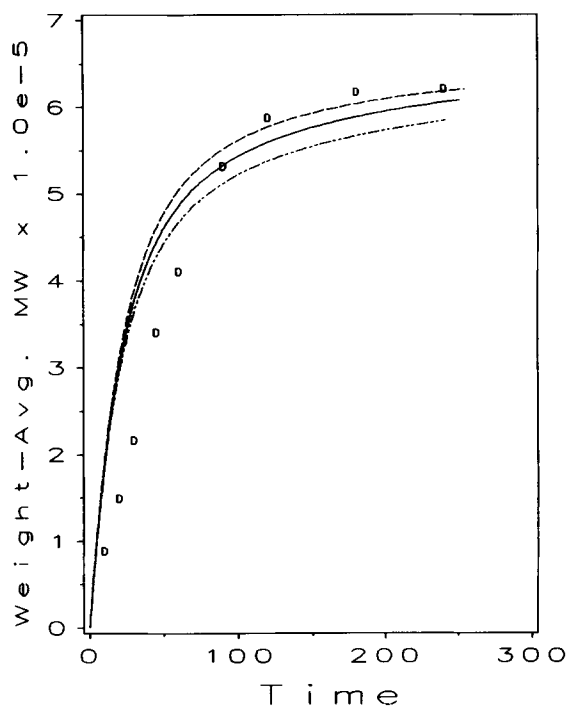


Figure 4 Weight-averaged molecular weight versus time for two active sites model for different values of FE. All other parameters are kept constant at $[Co] = 0.000125M$, $[M]_0 = 1.43M$, $T = 15^\circ C$, $F1 = 0.15$, $FFI = 2.25$, and $FFT = 1.0$: (D) M_w from experimental data (1); (---) M_w from simulation results for FE = 0.10; (—) M_w from simulation results for FE = 0.25; (- · - ·) M_w from simulation results for FE = 0.40.

ential equations which is shown in Table IV. Table IV also shows the initial condition.

The average rate constants are taken from Honig² as shown below:

$$k_p = (1.95 \times 10^9) \exp(-4570.6/T) \quad \text{L/mol min} \quad (40)$$

$$k_c = (2.82 \times 10^6) \exp(-5117.1/T) \quad \text{L/mol min} \quad (41)$$

$$k_b = 10^{-4} \quad \text{L/mol min (at } 15^\circ C) \quad (42)$$

$$k_t = 0.002 \quad \text{L/mol min (at } 15^\circ C) \quad (43)$$

The expressions for the rate constants for the two different sites are derived assuming the average rate constants above are actually composed of a weighted average of two individual rate constants for the two sites. For example, propagation is as follows:

$$k_p = F1 * k_{p1} + (1 - F1) * k_{p2} \quad (44)$$

where F1 = the fraction of active centers that are type 1

Defining

$$k_{p1} = \text{FFI} * k_p \quad (45)$$

where FFI = the multiplier for rate constant for site 1 for propagation, eq. (44) becomes

$$k_p = \text{F1} * \text{FFI} * k_p + (1 - \text{F1}) * k_{p2} \quad (46)$$

Solving for k_{p2} ,

$$k_{p2} = [(1 - \text{F1} * \text{FFI}) / (1 - \text{F1})] * k_p \quad (47)$$

Then eqs. (45) and (47) define k_{p1} and k_{p2} in terms of the average k_p and two adjustable parameters F1 and FFI.

Similar derivations were done for other reaction steps except it was not assumed that the multiplier FFI is the same for each reaction step. Instead a similar multiplier FFT is used for the chain transfer and deactivation steps:

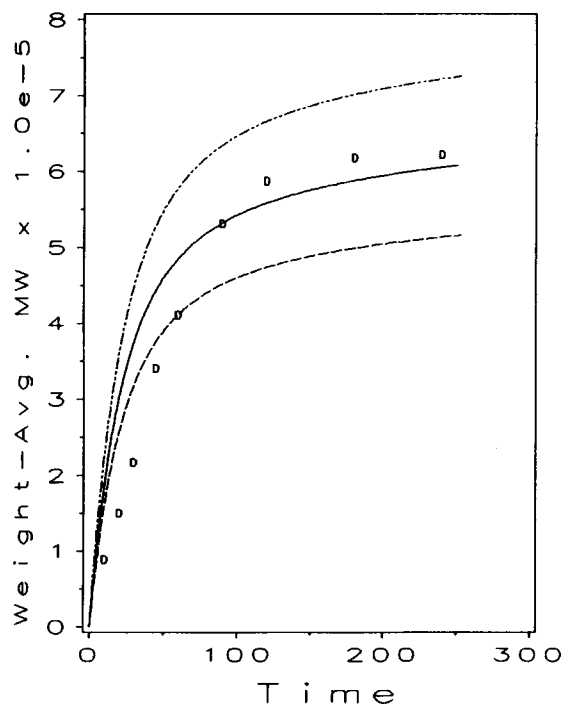


Figure 5 Weight-averaged molecular weight versus time for two active sites model for different values of F1. All other parameters are kept constant at $[\text{Co}] = 0.000125M$, $[\text{M}]_0 = 1.43M$, $T = 15^\circ\text{C}$, $\text{FE} = 0.25$, $\text{FFI} = 2.25$, and $\text{FFT} = 1.0$: (D) M_w from experimental data (1); (---) M_w from simulation results for $\text{F1} = 0.05$; (—) M_w from simulation results for $\text{F1} = 0.15$; (- · - ·) M_w from simulation results for $\text{F1} = 0.25$.

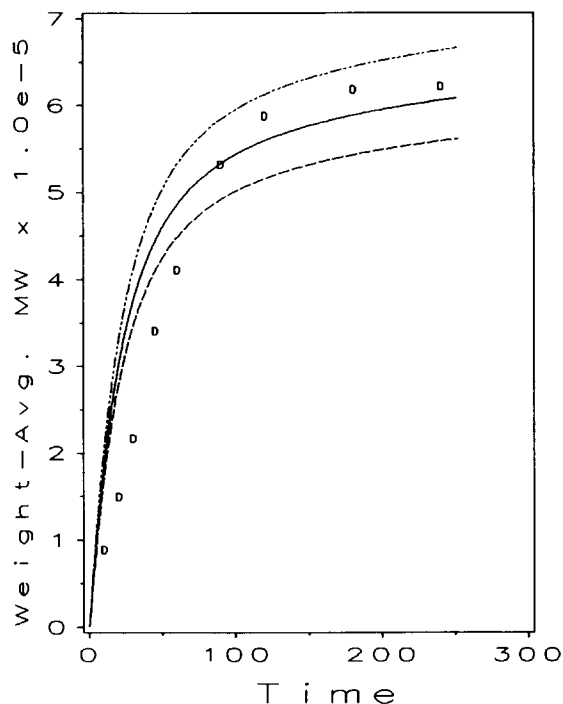


Figure 6 Weight-averaged molecular weight versus time for two active sites model for different values of FFI. All other parameters are kept constant at $[\text{Co}] = 0.000125M$, $[\text{M}]_0 = 1.43M$, $T = 15^\circ\text{C}$, $\text{FE} = 0.25$, $\text{F1} = 0.15$, and $\text{FFT} = 1.0$: (D) M_w from experimental data (1); (---) M_w from simulation results for $\text{FFI} = 2.00$; (—) M_w from simulation results for $\text{FFI} = 2.25$; (- · - ·) M_w from simulation results for $\text{FFI} = 2.50$.

$$k_{c1} = \text{FFT} * k_c \quad (48)$$

$$k_{c2} = \{ [1 - (\text{F1} * \text{FFT})] / (1 - \text{F1}) \} * k_c \quad (49)$$

$$k_{b1} = \text{FFT} * k_b \quad (50)$$

$$k_{b2} = \{ [1 - (\text{F1} * \text{FFT})] / (1 - \text{F1}) \} * k_b \quad (51)$$

$$k_{t1} = \text{FFT} * k_t \quad (52)$$

$$k_{t2} = \{ [1 - (\text{F1} * \text{FFT})] / (1 - \text{F1}) \} * k_t \quad (53)$$

RESULTS AND DISCUSSION

In Honig's article the initiation rate constant (k_i) is set to a large number because in the system under study, an induction or acceleration period was not observed. Therefore, the initiation is instantaneous. Because of this, in the computer simulation, the initiation for formation of the active site step is omitted in the system of differential equations. However, the initial condition is set corresponding to the assumption that all the catalyst has formed active sites

or died. (Note: The initial conditions are described in Table IV.)

In the dual active site model proposed, since there are two different values of rate constants for each step (one each for each type of active site) and the average value of the rate constant for each step is the same as the values mentioned above, some parameters are needed. Each parameter has its own effects. To see the effect of FE (fraction of all Co that forms active centers), three different values of FE are assumed and all other parameters are kept constant. Figures 2, 3, and 4 show the effects of different values of FE. It is found out that the fewer the active centers formed, the lower the conversion. Also, it is found out that for fewer active centers formed, the molecular weight will be higher.

The different values of parameter F1 (fraction of active centers that has first type of active site) when all other parameters are kept constant have little effect on conversion and number-averaged molecular weight. However, the value of F1 has a significant effect on weight-averaged molecular weight. The

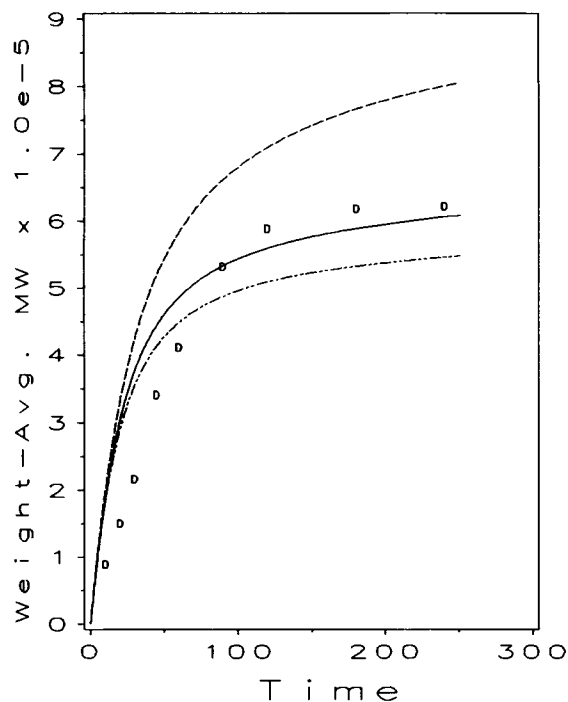


Figure 7 Weight-averaged molecular weight versus time for two active sites model for different values of FFT. All other parameters are kept constant at $[Co] = 0.000125M$, $[M]_0 = 1.43M$, $T = 15^\circ C$, $F1 = 0.15$, and $FFI = 2.25$: (D) M_w from experimental data (1); (---) M_w from simulation results for $FFT = 0.60$; (—) M_w from simulation results for $FFT = 1.00$; (- · -) M_w from simulation results for $FFT = 1.40$.

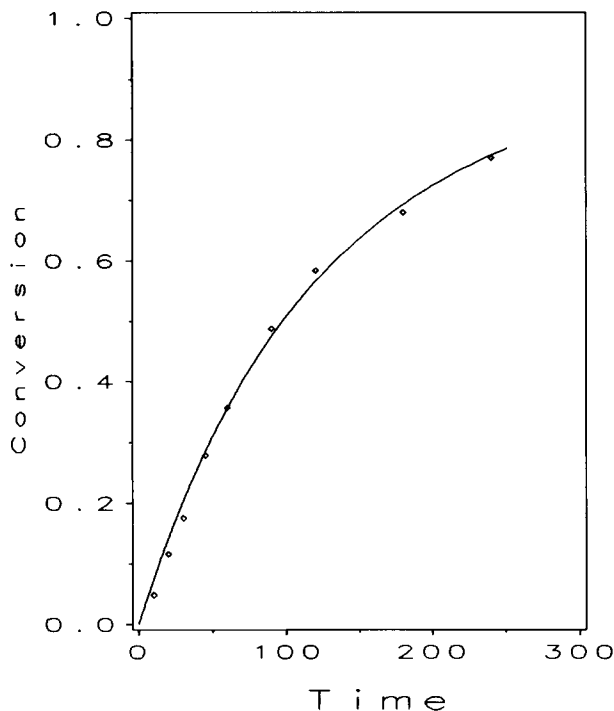


Figure 8 Conversion versus time for two active sites model for $[Co] = 0.000125M$, $[M]_0 = 1.43M$, $T = 15^\circ C$, $FE = 0.25$, $F1 = 0.15$, $FFI = 2.25$, and $FFT = 1.0$: (\diamond) conv. from experimental data (1); (—) conv. from simulation results.

fewer the first type of active center formed (the first type corresponds to the one that has faster rate in propagation step), the lower the weight-averaged molecular weight. Figure 5 clearly shows this phenomenon.

The values of the multiplier for the first type of active site for propagation step (FFI) have very little or no effect on conversion and number-averaged molecular weight but have a significant effect on weight-averaged molecular weight. Figure 6 shows that the lower the value of the FFI, the lower the weight-averaged molecular weight. This trend is true until the value of FFI is equal to 1. Further decrease in the value of FFI will make k_{p2} become greater than k_p . Therefore, the weight-averaged molecular weight will increase again.

Lastly, Figure 7 shows the effect of the multiplier for first type of active site for other than propagation step (FFT). When the value of FFT is lowered, the weight-averaged molecular weight is increased.

After trial and error as indicated above, a good match between simulation and experimental results was obtained from the following combination of the values for the parameters.

$$FE = 0.25$$

$$F1 = 0.15$$

$$FFI = 2.25$$

$$FFT = 1.00$$

The results from dual site model are shown in Figures 8, 9, and 10. In Figure 8, a plot of simulation result for conversion versus time matches to the experimental results obtained from Honig's dissertation. Figures 9 and 10 show the molecular weights versus conversion and time, respectively. From these figures, it can be shown that the match is much better than the single site model shown in Figure 1. Both number and weight average molecular weights curves show good agreement to the experimental results. This improved fit of the model predictions with

the experimental data, especially the weight-averaged molecular weight, indicates that a model based on the two site mechanism could be used for design purposes. However, a two site mechanism is yet to be proven based on the catalytic mechanism study.

CONCLUSION

A proposed mathematical model based on a polymerization mechanism that involves dual active sites has been derived. The adequacy of this model has been tested with the data obtained in the literature and the model is found to be adequate for predicting the molecular weights and conversion trends in the polymerization of butadiene using cobalt octoate/diethyl aluminum chloride catalyst system. Further

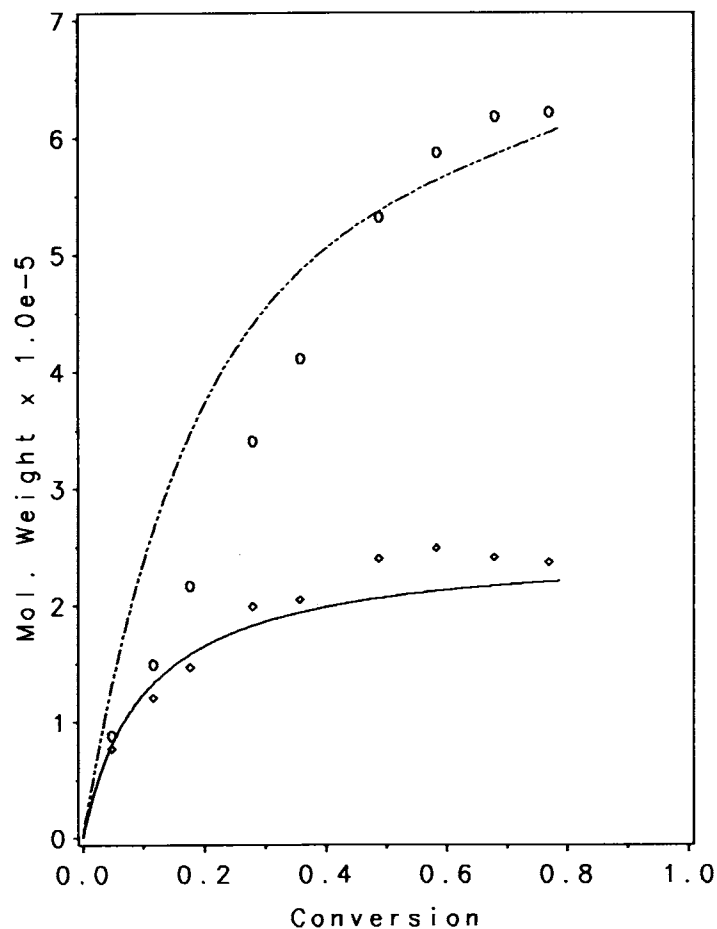


Figure 9 Molecular weights versus conversion for two active sites model for $[Co] = 0.000125 M$, $[M]_0 = 1.43 M$, $T = 15^\circ C$, $FE = 0.25$, $F1 = 0.15$, $FFI = 2.25$, and $FFT = 1.0$: (O) M_w from experimental data (1); (◇) M_n from experimental data (1); (---) M_w from simulation results; (—) M_n from simulation results.

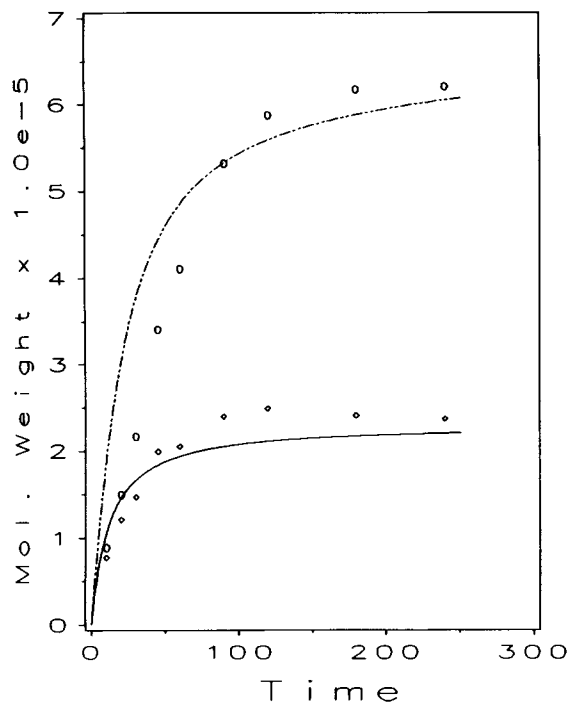


Figure 10 Molecular weights versus time for two active sites model for $[Co] = 0.000125 M$, $[M]_0 = 1.43 M$, $T = 15^\circ C$, $FE = 0.25$, $F1 = 0.15$, $FFI = 2.25$, and $FFT = 1.0$: (\circ) M_w from experimental data (1); (\diamond) M_n from experimental data (1); (- · - ·) M_w from simulation results; (—) M_n from simulation results.

proof for the formation of two active sites would be an interesting subject for future study.

REFERENCES

1. J. A. J. Honig, Dissertation, University of New South Wales, Sydney, Australia (1985).
2. J. A. J. Honig, P. E. Gloor, J. F. MacGregor, and A. E. Hamielec, *J. Appl. Polym. Sci.*, **34**, 829 (1987).
3. C. C. Hsu and L. Ng, *AIChE J.*, **22**(1), 66 (1976).
4. W. L. Yang and C. C. Hsu, *J. Appl. Polym. Sci.*, **28**, 145 (1983).
5. F. K. W. Ho, C. C. Hsu, and D. W. Bacon, *J. Appl. Polym. Sci.*, **32**, 5287 (1986).
6. J. A. J. Honig, R. P. Burford, and R. P. Chaplin, *J. Polym. Sci. Polym. Chem. Ed.*, **21**, 2559 (1983).
7. Dong-Ho Lee and C. C. Hsu, *J. Appl. Polym. Sci.*, **25**, 2373 (1980).
8. Dong-Ho Lee and C. C. Hsu, *J. Appl. Polym. Sci.*, **26**, 653 (1981).
9. S. S. Medvedev (dec.), L. A. Volkov, V. S. Byrikhin, and G. V. Timofeyeva, *Polym. Sci. U.S.S.R.*, **13**(6), 1561 (1971).
10. John James Roffel, Thesis, McMaster University, Hamilton, Ontario (1990).
11. Michael L. Michelsen, *AIChE J.*, **22**(3), 594 (1976).

Received December 20, 1990

Accepted April 17, 1991